Medicine and Medical Sciences 12(1): 001-011, February 2024
DOI: 10.15413/mms.2024.0100
ISSN 2682-5759

Academia Publishing

Research Paper

Improved prediction of bone mechanical parameters based on clinically available CT data

Accepted 8th January, 2024

ABSTRACT

The goal of all studies relating bone density and structure to bone strength is to predict fracture risk in a specific patient using clinically available data. The aim of the present study was to test a new method to describe the mechanical properties of bone using clinically available data and to compare it with routine procedures. The study was performed on 50 L3 vertebrae taken from males aged 22 to 81 years. The samples were examined with dual-energy X-ray absorptiometry and quantitative CT. An extensive analysis was carried out for 2-dimensional (2D) and 3-dimensional(3D) CT images. Also, a 2D image histogram analysis was performed. The parameters(mean – XC_1/XC_2, standard deviation – SD_1/SD_2, and area – X_1/X_2)characterizing the organic matrix and bone material were calculated by fitting two Gaussian functions. The compression test was performed to determine ultimate stress (σ_{max}), ultimate strain, elastic modulus (E), and the ratio of work to fracture and the volume of the vertebra. The study carried out made it possible to determine several dozens of parameters that describe the geometry, architecture, density, and mechanical properties of the vertebral body. It was found that E and σ_{max} was best described by the parameter related to trabecular bone density (XC_2) obtained from the histogram analysis. The adjusted coefficient of determination (R^2) is equal to 0.688 and 0.836 for E and σ_{max}, respectively. For volumetric/areal bone mineral density (vBMD/aBMD), R^2 is 0.619/0.159 for E wile for σ_{max} equals to 0.771/0.316. It is also possible to correct the vBMD using histogram parameters. The R^2 values for E and σ_{max} rise to 0.673/0.825 after the correction. The superiority of a new method of E and σ_{max} assessment using clinically available CT data was confirmed. The proposed method does not require calibration and predicts the mechanical parameters of the vertebrae more precisely than vBMD/aBMD. In addition, it can be implemented in the opportunistic analysis of CT data.

Key words: Human vertebra, CT examination, Image histogram analysis, prediction of mechanical properties, opportunistic screening.

E. Rokita[1,2*], A. Wróbel[2] and G. Tatoń[1]

[1]Department of Biophysics, Jagiellonian University Medical College, Św. Łazarza 16, 31530 Kraków, Poland.
[2]Institute of Physics, Jagiellonian University, S. Łojasiewicza 11, 30348 Kraków, Poland.

*Corresponding author. E-mail:eugeniusz.rokita@uj.edu.pl. Tel: +48-12-6199680. Fax: +48-12-6199685

Abbreviations: 2D/3D, Two-/three-dimensions; **aBMD,** Areal BMD; **AIC,** Akaike information criterion; **BIC,** Bayesian information criterion; **BMD,** Bone mineral density; **BV/TV,** Bone volume/total volume; **DXA,** Dual-energy X-ray absorptiometry; **E,** Elastic modulus; **FE,** Finite element method; **FR,** Fracture risk; **GL,** Grey level; **GLC,** GL inside spinous process; **GLT,** GL of trabecular bone; **p,** Significance level; QCT, Quantitative computed tomography; r, Correlation coefficient; R^2, Coefficient of determination; **RGL,** Relative GL; **ROI,** Region of interest; **SD,** Standard deviation; **U/V,** Work to fracture/volume of the vertebral body; **vBMD,** Volumetric BMD; $\mathbf{X_i}$, Normalized volume fraction; $\mathbf{XC_i}$, Parameter linearly related to density; $\boldsymbol{\varepsilon_{max}}$, Ultimate strain; $\boldsymbol{\sigma_{max}}$, Ultimate stress.

INTRODUCTION

Bone fractures represent a significant cause of disability and loss of quality of life among the elderly population. Therefore, proper evaluation of bone mechanical parameters and determination of risk of fracture (FR) are an important issue (Kanis et al., 2019; Tarantino et al., 2017). Direct measurement of bone mechanical properties is not possible in clinical practice; the mechanical strength of bone must be estimated indirectly. The standard diagnostic approach, unchanged for several decades, consists of determining the areal bone mineral density (aBMD) and comparing the results with the values of the young population (T-score).

Since aBMD-based test can only provide a rough understanding of how much weaker bones have become, numerous attempts have been made to develop more accurate diagnostic methods. Trials have been carried out to replace or supplement aBMD determinations with measurements of the geometry, microarchitecture, and volumetric BMD (vBMD) of bones using quantitative computed tomography (QCT), peripheral QCT, high-resolution magnetic resonance imaging, micro-CT, or a combination of these methods (Leslie et al., 2018; Nethander et al., 2020; Shepherd et al., 2015; Silva et al., 2015; Lopez Picazo et al., 2019; Soldati et al., 2021; Hutchinson et al., 2017; Krug et al., 2010). Another approach (Lopez et al., 2012; Dall'Ara et al., 2012) is based on bone strength calculations using the finite element method (FE). To perform the FE simulations, both micro- and macro-mechanical models are constructed using CT data. Recently, radiomic features of CT images and artificial intelligence-based image analyses have also been used to differentiate between normal and pathologically altered bones (Xie et al., 2022; Yan et al., 2023).

Based on the authors' knowledge, none of the diagnostic approaches described above have been widely accepted in clinical practice. The question arises whether it is possible to determine the mechanical parameters of the bones more precisely than the methods currently used based on clinically available CT data. It is also important to be able to use CT examinations for bone diagnostics, which were performed to solve other diagnostic problems (opportunistic analysis).

The purpose of this study is to test a new method to describe the mechanical properties of bones based on clinically available CT data. The usefulness of the method for opportunistic CT data analysis is also discussed.

MATERIALS AND METHODS

The study comprises a reanalysis of preexisting data acquired in previous experiments (Tatoń et al., 2012; Tatoń et al., 2013 a, b; Tatoń et al., 2014). Approval for this reanalysis was not necessary due to the retrospective and de-identified nature of the data. For the primary investigation, 50 cadaveric L3 vertebrae obtained from males aged 22 to 81 years were used. The material tested was limited to male vertebra samples to exclude gender-specific impacts on BMD (Alswat, 2017). The deaths resulted from various causes. The main causes were cardiogenic diseases and cerebrovascular attacks. All cadavers were included without bone disease screening because a complete medical history was not available for all subjects.

The following is a brief description of the experiment originally performed. Immediately after removal, the samples were placed in the methacrylate body phantom filled with 0.9% NaCl solution to stimulate physiological conditions. The samples were examined with dual-energy X-ray absorptiometry (DXA) using a Lunar DPX-IQ densitometer (Lunar, Madison, USA), following standard procedures applied for humans. A Siemens Somatom Sensation 10 CT unit (Siemens, Erlangen, Germany) was used for CT examinations (120 kV, 120 mAs, slice thickness: 0.6 mm). A 75×75 mm^2 region of interest (ROI) and a matrix of 512·512 resulted in a pixel size of 146·146 μm^2 in the plane of the scan. CT data was also used to determine the BMD of the trabecular bone region (vBMD) within the vertebral bodies. The Siemens Osteo-CT procedure (Siemens, Erlangen, Germany) was applied for the determination of vBMD.

Two-dimensional (2D) CT images were applied to perform a quantitative characterization of the trabecular bone architecture within ROI^T (Figure 1). An in-house code was developed to perform the calculations. Based on our previous results (Tabor and Rokita, 2000; Kubik et al., 2002; Tabor, 2009), the architecture description was limited to one parameter (bone volume/total bone volume - BV/TV), although a total of ~30 quantities were tested.

Finally, DICOM data acquired in CT examinations were reconstructed in 3 dimensions (3D), using software developed in our laboratory. 3D images were used to measure the linear, areal, and volumetric dimensions of vertebral bodies (Tatoń et al., 2013a). Subsequently, 3D images were applied to identify vertebral fractures according to the method of Genant et al. (1993).

After CT scans, all specimens were subjected to axial compression to failure on an Instron 5566 testing machine (Instron, High Wycombe, UK)(Tatoń et al., 2013b; Tatoń al., 2014). Briefly, after preconditioning, each sample was compressed to failure at a strain rate of 5 mm/min. The description of the parameters determined is given in Appendix 1.

As the new step in 2D image analysis (Figure 1), the grey level (GL) histogram was constructed for ROI^T (GLT). The histogram was normalized using the average GL within ROI^{IS}(<GLC>) and the relative grey level histogram (RGL = GLT/<GLC>) was computed. ROI^T and ROI^{IS} were manually

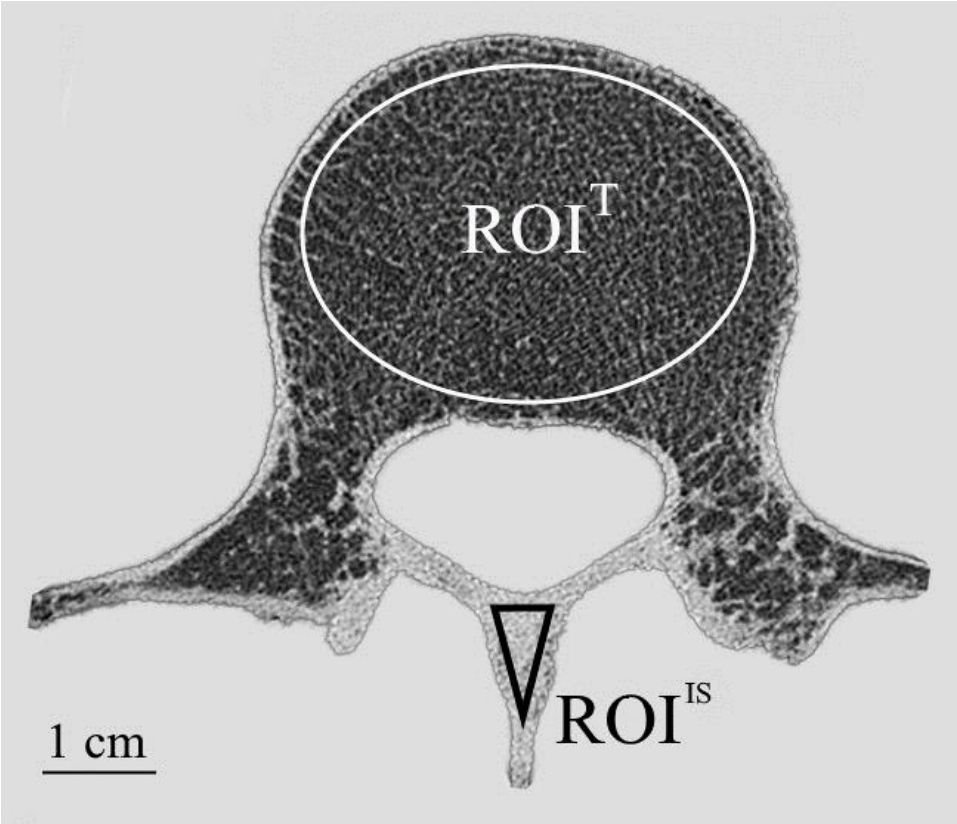

Figure 1: Representative 2D CT image of human vertebral cross sections. The regions of interest used for the calculation of trabecular bone parameters (ROI^T) and for normalization of the ROI^T histogram (ROI^{IS}) are marked.

selected by placing an ellipse and a triangle in the body and the spinous process of the vertebra, respectively. Thereafter, all RGL histograms (~40 sections for each vertebra) were pooled together and the global histogram for the vertebral body was prepared. The global histogram was normalized (area = 1) and the average grey level was calculated (<RGL>). Finally, two Gaussian functions were fitted (Figure 2). By applying this method, the global histogram was decomposed into two different classes, hereinafter referred to as the organic matrixand bone material (Appendix 2). Five parameters (mean – XC_1/XC_2, standard deviation – SD_1/SD_2, area – X_1/X_2) were obtained. The indices '1' and '2' mark the organic matrix and bone material, respectively. It should be emphasized that due to the normalization of the histogram, $X_1 + X_2 = 1$. Therefore, the number of independent parameters is five.

It should be noted that ROI^T of a 2D image (Figure 1) contains $\sim 2 \cdot 10^4$ pixels. Therefore, the global histogram for a vertebral body (Figure 2) comprises several hundred thousand points. The histogram skewness is positive in all cases and ranges from 0.26 to 1.19. Therefore, two Gaussian distributions were fitted to reproduce the experimental data. Unambiguously, fitting the two Gaussian curves provides an excellent reproduction of the experimental data ($R^2 > 0.999$).

Results are presented as parameter ranges, and as mean±SD. Relationships between parameters and age were investigated using the Pearson correlation coefficient (r) and its significance level(p). The statistical significance of the differences in the correlation coefficients was tested using the procedure proposed by Steiger (1980). The Student t-test was applied to compare mean values. Different regression models (linear – ax +b, parabolic – ax^2+bx+c, logistic – $a/(1 + b \cdot \exp(-cx))$, power – ax^b,) were constructed for the selection of variables explaining mechanical tests. Single or two predictor models were tested. The best model was selected using the adjusted coefficient of determination value(R^2), as well as the AIC (Akaike Information Criterion) and BIC (Bayesian Information Criterion) tests. OriginPro 2020 software (Northampton, Massachusetts, USA) was used to perform statistical analysis.

RESULTS AND DISCUSSION

The main aim of the studies was to improve description of the mechanical properties of the vertebra (FR prediction) based on the available clinical data. The conducted research allowed to determine several dozens of parameters

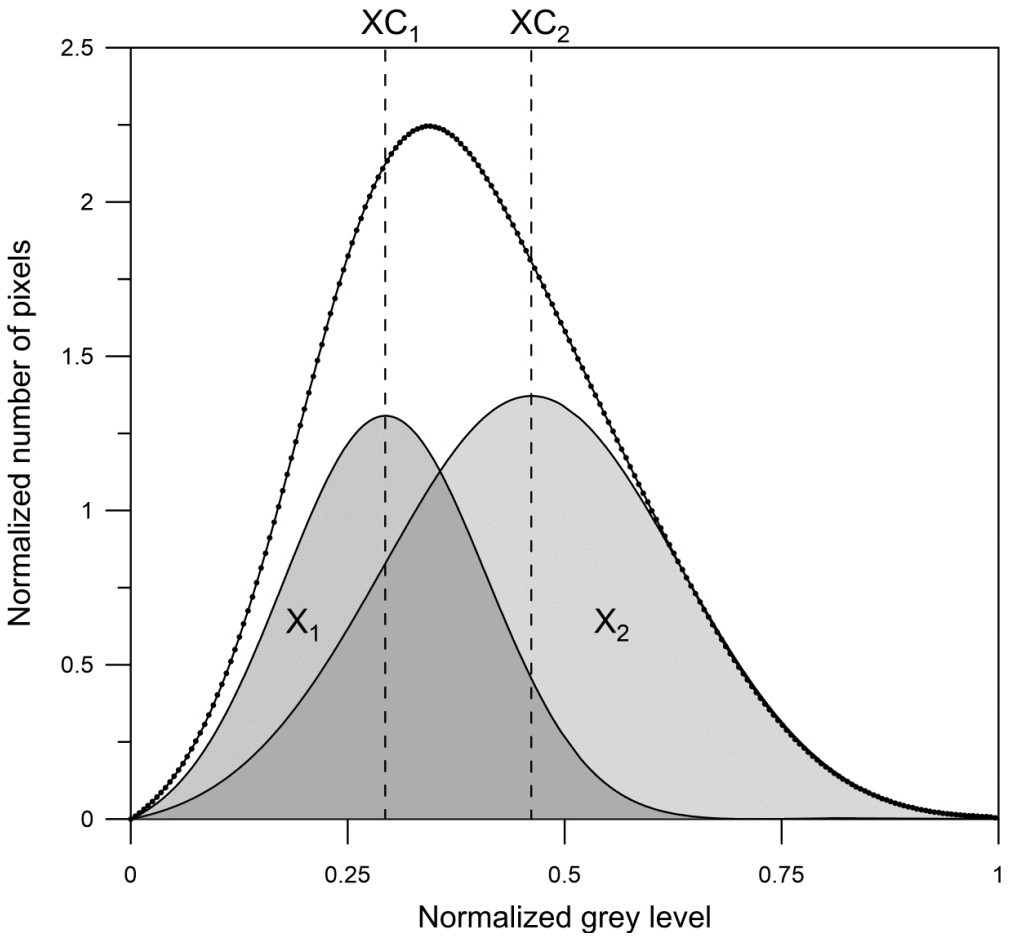

Figure 2: Example of the normalized global histogram of the relative grey level distribution for a vertebral body. X_1 and X_2 are the areas and XC_1 and XC_2 mark the positions of the maxima of 2 Gaussian functions. The black dots represent experimental points (every second point is shown). The sum of 2 Gaussian functions (solid line) perfectly reproduces the experimental points ($R^2 = 0.9997$).

describing the geometry, architecture, density, and mechanical properties of the vertebral body. Therefore, it is necessary to adopt a criterion that allows the initial selection of experimental data.

Furthermore, it is well known that FR depends on pathological changes and age-related physiological alterations (Demontiero et al., 2012; Boskey and Coleman, 2010). In the study, it is assumed that the natural ageing process is observed in the absence of fractures, since the bone fracture changes the parameters values in a way that is impossible to quantify. As a result, it was decided to determine the relationship between mechanical parameters and clinical data only for unbroken vertebrae. According to the Genant classification (1993), vertebrae with mild (grade 1) or larger deformities were considered as fractured. It should be noted that Genant approach is based on both visual classification by two radiologists and quantitative morphometric measurements. The visual analysis of the 2D images showed that for some subjects, the images differ significantly from the standard cases (Figure 3A and B). For example, in Figure 3C the difference is clearly visible even without quantitative analysis. The vertebra with severe degenerative changes (e.g. Fig. 3C) was not included in the data analysis. In the group of 50 cases studied, 18 did meet the selection criterions. The use of stringent criteria limited the size of the study group but ensures that the group for which there are only physiological changes depending on age is analyzed.

Moreover, it is well known that the mechanical strength of bones decreases with age (Demontiero et al., 2012; Boskey and Coleman, 2010). To describe the mechanical parameters by the available clinical quantities, one should use those clinical data that change with age. Therefore, in studies, the correlation criterion with age has been adopted for the selection of parameters. When selecting parameters, one should also remember the multicollinearity effect.

Table 1 shows the ranges of selected parameters and their correlations with age. Among the parameters that characterize the mechanical properties of vertebrae, σ_{max}, E and U/V correlate with age. For ultimate strain (ε_{max}), the

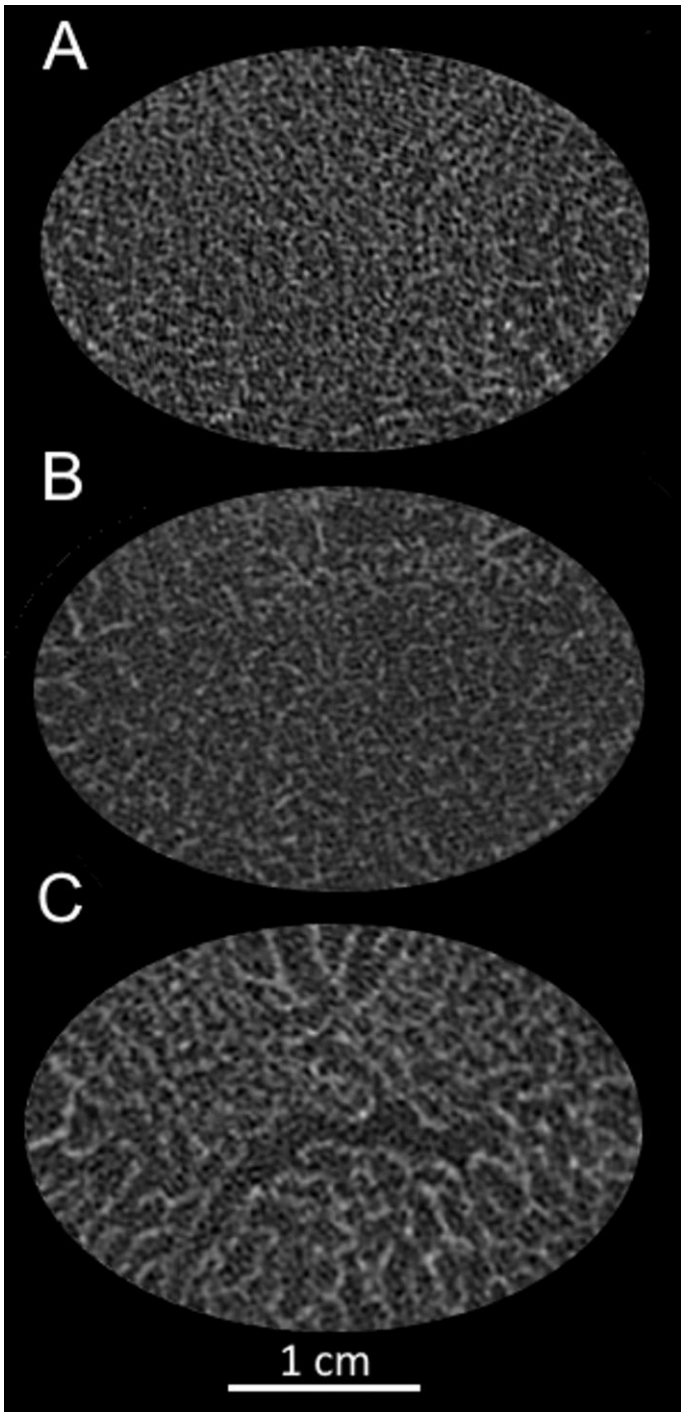

Figure 3: 2D CT images of the ROI^T regions for human L3 vertebral bodies collected from 25 (A), 66 (B), and 24 (C) year-old subjects.

correlation is not observed (r = -0.38, p= 0.115). It should be noted that there is no commonly accepted method of assessing fracture risk (Diacinti and Guglielmi, 2019; Lentle et al., 2019). In our study, it was assumed that the most important parameter characterizing the FR is σ_{max}, as it denotes when fractures really do occur. With E in addition, it is possible to estimate the values of U/V and ε_{max} (Appendix 1). The selection of parameters matches the widely accepted opinion that strength (σ_{max}) and stiffness (E) are the best quantities to define the "health" of bone. The values of σ_{max} and E (Table 1) are in line with those previously published (Karim et al., 2013; Boskey and Imbert, 2017). Furthermore, there are significant differences for young (≤ 55 y) and old (> 55 y) individuals in the case of average σ_{max} (11.4 ± 2.0 vs 6.81 ± 2.59 MPa, p=0.0005) and E (326 ± 36 vs 202 ± 70 MPa, p=0.0002).

Regarding the vertebral geometry, data analysis confirms a general regularity. The L3 vertebrae show a trend towards a decrease in all height values (H) and an increase in axial cross-sectional areas(A) with age, while the volume (V) of the body does not change with age (r = 0.22, p= 0.382). The description of the influence of the geometry of the lumbar vertebra on the mechanical parameters was previously carried out (Tatoń et al., 2013a), this problem will not be discussed in detail in this study. Briefly, differentiation of broken/unbroken vertebrae may be accomplished by applying vertebral geometry. It does not provide information on the mechanical parameters of the unbroken vertebrae.

Most of the parameters that characterize the minerality of avertebral body correlate with age. This applies both to 3 parameters obtained from histogram analysis (X_2, XC_2, SD_2) and to the parameters commonly used in the description of trabecular bone density (vBMD) or to the parameter related to bone density (BV/TV). Unlike bone material, the parameters that characterize the organic matrix (XC_1, SD_1) vary to a very narrow extent (0.29 ÷ 0.35 and 0.08÷ 0.12, respectively) and do not correlate with age (r = -0.46, p= 0.057 and r = -0.27 p= 0.271, respectively). XC_1 and SD_1 are also not correlated (r = 0.006, p = 0.982). It should be emphasized that aBMD does not correlate with age in cases without fracture. This parameter will be further considered, as it is the most widely used to assess fracture risk in clinical practice.

As the first step in describing the mechanical parameters by CT data, a linear regression model was used. The correlations between mechanical parameters and selected vertebral body parameters that are clinically available are given in Table 2. Table 2 does not contain U/V (Appendix 1) while the parameter vBMD/X_2 (Appendix 2) was also included. The values given in Table 2 confirm the positive proportionality of different measures of the bone mineral density with bone strength and stiffness, what has been repeatedly demonstrated over many years. It should be noted that the obtained results prove that XC_2 and vBMD/X_2 are the best predictors of the mechanical parameters of the vertebrae.

In the next step, to describe the relationship between mechanical parameters and predictor variables whist taking away the effect of age on the relationship, the partial correlations were calculated. The data in Table 3 confirm that XC_2 and vBMD/X_2 are the best predictors of the mechanical parameters.

Table 1: The ranges of values of the parameters describing selected properties the of L3 vertebral body. The correlationsof parameters with age (r) and pvalue are given.Abbreviations: σ_{max} – ultimate stress (MPa), E – elastic modulus (MPa), U/V – the ratio of the work to fracture and the vertebra volume (MPa), A – the area of the axial cross section at the narrowest site of the of the vertebral body (cm^2), H – the average height of the vertebral body (cm), BV/TV – bone volume/total volume, vBMD – volumetric bone mineral density (g/cm^3), aBMD – areal bone mineral density (g/cm^2), X_2, XC_2, SD_2 – area, mean and standard deviation of the Gaussian function representing the bone material.

Parameter	Range	r	p
σ_{max}	3.83 ÷ 13.8	-0.74	<0.001
E	141 ÷ 394	-0.77	<0.001
U/V	0.11 ÷ 0.41	-0.64	0.005
A	10.9÷18.2	0.75	<0.001
H	1.97÷3.05	-0.74	<0.001
BV/TV	0.09 ÷ 0.30	-0.71	0.001
vBMD	0.051 ÷ 0.169	-0.65	0.004
aBMD	0.74 ÷ 1.53	-0.40	0.110
X_2	0.39 ÷ 0.72	-0.55	0.018
XC_2	0.31 ÷ 0.62	-0.69	0.001
SD_2	0.12 ÷ 0.17	-0.75	<0.001

Table 2: Linear regression model fitting results. Correlations between 2 mechanical parameters and parameters characterizing the density of the L3 vertebral body. The values of the correlation coefficient and pare given. Abbreviations: E – elastic modulus, σ_{max} – ultimate stress, BV/TV – bone volume/total volume, vBMD – volumetric bone mineral density, aBMD – areal bone mineral density, X_2, XC_2, SD_2 – area, mean and standard deviation of the Gaussian function representing bone material.

Parameter	E	σ_{max}	BV/TV	vBMD	aBMD	X_2	XC_2	SD_2
σ_{max}	0.89 <0.001	1						
BV/TV	0.75 <0.001	0.85 <0.001	1					
vBMD	0.80 <0.001	0.89 <0.001	0.79 <0.001	1				
aBMD	0.46 0.057	0.60 0.009	0.52 0.028	0.80 <0.001	1			
X_2	0.56 0.015	0.65 0.004	0.67 0.002	0.85 <0.001	0.74 <0.001	1		
XC_2	0.84 <0.001	0.92 <0.001	0.78 <0.001	0.90 <0.001	0.66 0.003	0.65 0.004	1	
SD_2	0.79 <0.001	0.82 <0.001	0.77 <0.001	0.77 <0.001	0.59 0.009	0.65 0.004	0.74 0.001	1
vBMD/X_2	0.83 <0.001	0.91 <0.001	0.74 0.001	0.88 <0.001	0.67 0.002	0.59 0.011	0.92 <0.001	0.73 0.001

Table 3: Partial correlations (effect of age has been removed) between mechanical parameters and parameters characterizing the density of the L3 vertebral body. The values of the partial correlation coefficient and pare given. Abbreviations: E – elastic modulus, σ_{max} – ultimate stress, BV/TV – bone volume/total volume, vBMD – volumetric bone mineral density, aBMD – areal bone mineral density, X_2, XC_2, SD_2 – area, mean and standard deviation of the Gaussian function representing bone material.

Parameter	E	σ_{max}	BV/TV	vBMD	aBMD	X_2	XC_2	SD_2
σ_{max}	0.75 0.001	1						
BV/TV	0.44 0.077	0.69 0.001	1					
vBMD	0.62 0.008	0.79 <0.001	0.61 0.010	1				
aBMD	0.26 0.315	0.49 0.045	0.37 0.146	0.77 <0.001	1			
X_2	0.26 0.311	0.43 0.085	0.48 0.049	0.78 0.0002	0.68 0.003	1		
XC_2	0.67 0.004	0.84 <0.001	0.56 0.019	0.82 <0.001	0.59 0.013	0.68 0.003	1	
SD_2	0.49 0.046	0.60 0.010	0.51 0.035	0.57 0.017	0.49 0.046	0.42 0.092	0.44 0.074	1
vBMD/X_2	0.71 0.001	0.86 <0.001	0.54 0.024	0.87 <0.001	0.59 0.012	0.38 0.138	0.86 <0.001	0.51 0.037

The obtained results clearly confirm that aBMD does not offer a good assessment of the mechanical parameters (Tables 2 and 3). In contrast to aBMD, vBMD provides better prediction of the mechanical parameters. Determining vBMD requires a CT scan, which significantly limits the use of this parameter in clinical practice. It should also be noted that the prediction of osteoporosis using aBMD and vBMD does not overlap. According to the criteria of aBMD for the diagnosis of osteoporosis (T-score < - 2.5) (Kanis et al., 2019), samples subjected to studies can be classified as normal/osteopenic (15 cases) and osteoporotic (3 cases). Using the vBMD values (< 0.080 g/cm^3) for classification (American College of Radiology, 2013), we get 13 and 5 cases, respectively.

In many studies, the quantities that characterize the vertebral microstructure are also calculated based on clinical CT data (Yamada et al., 2019; Akhter and Recker, 2021). This approach is in line with the commonly accepted opinion that to fully characterize the mechanical properties of vertebrae, it is necessary to supplement density measurements with a quantitative description of the trabecular architecture (Karim et al., 2013). However, in clinical practice, the parameters that characterize the architecture of the trabecular bone are not used. The basic problem of bone microstructure studies is the problem of the resolving power of CT images obtained in clinical trials (Kim et al., 2004; Tatoń et al., 2012; Liu et al., 2020). Although modern CT scanners achieve an isotropic resolution of ∼0.5 mm (Engelke, 2017), for standard clinical examination, a minimum in-plane resolution of the order of 1 mm and a slice thickness > 1 mm are used. Hence, given typical dimensions of trabeculae, the image resolution seems to be the borderline for a quantitative determination of trabecular architecture.

The common feature of all methods currently tested to replace or supplement density measurements is that instead of directly measuring microstructural parameters, there is a tendency to use textural descriptors to characterize the trabecular architecture without requiring stringent segmentation of the individual trabecula (Checefsky et al., 2016; Gebre et al., 2021; Valentinitschl et al., 2019). Similarly, texture analysis can be applied to DXA images by computing the trabecular bone score (TBS)(Silva et al., 2015). More computer-advanced studies of trabecular architecture measurements from DXA-derived 3D models have been published (Lopez Picazo et al., 2019). Recently,

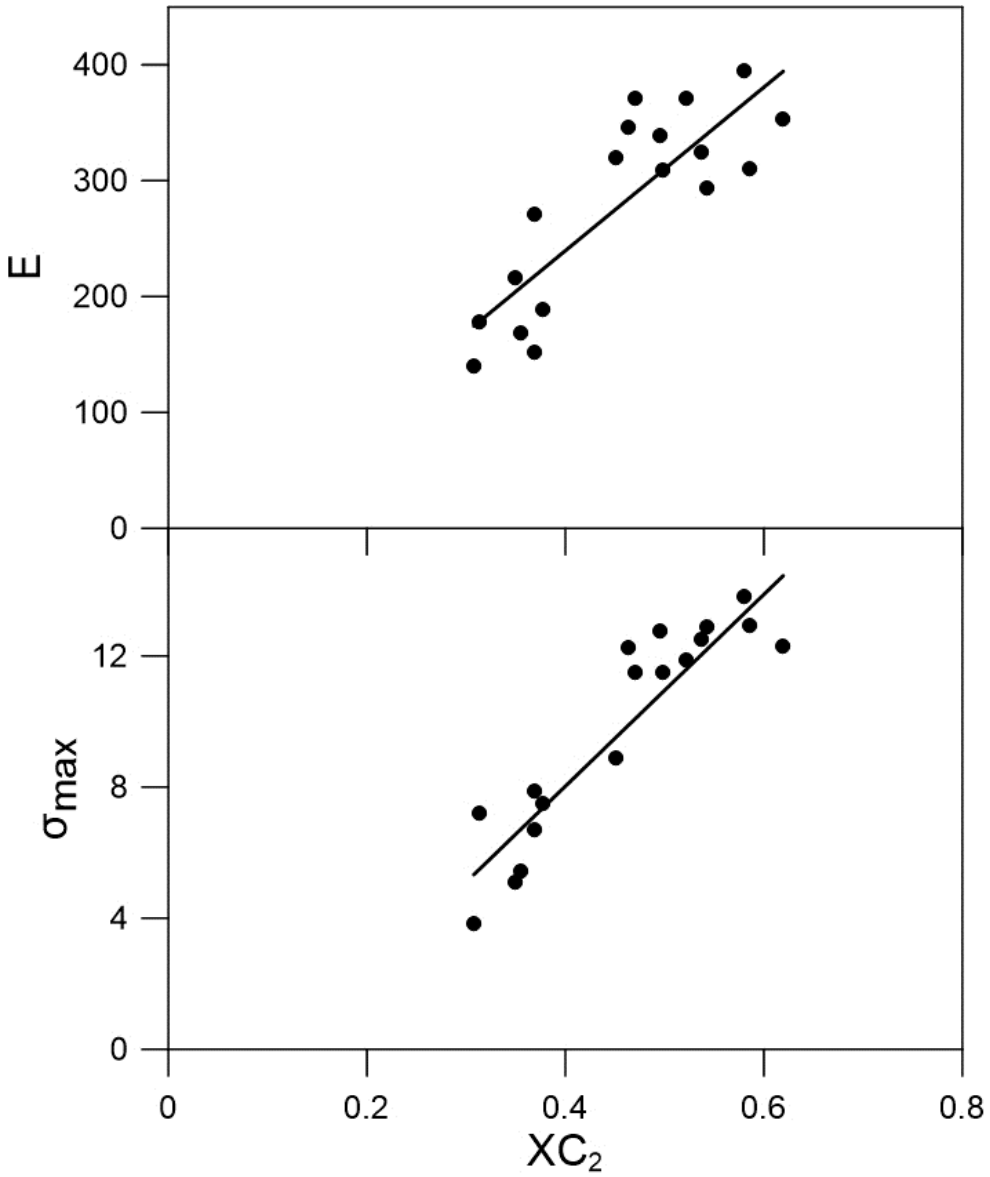

Figure 4: Elastic modulus (E - MPa) and ultimate stress (σ_{max} - MPa) vs bone material density measure (XC_2) extracted from histogram analysis. Solid line represents the linear regression model (R^2 = 0.688 and 0.836 for E and σ_{max}, respectively).

attempts had also been made to take advantage of radiomic features for FR assessment (Xie et al., 2022; Xue et al., 2022). It should be noted that the texture analysis is based on the quantitative description of image grey-level variations without biophysical background. In our study, we proposed a new, very simple method instead of density determination or texture analysis.

In our approach, the quantitative description of trabecular bone density is based on image histogram analysis. The proposed histogram analysis allows for the separation of the organic matrix and bone material. The determined parameter (XC_2) is related to bone density and allows the best prediction of the mechanical parameters of all thequantities tested. Figure 4 shows the modulus of elasticity (E) and ultimate stress (σ_{max}) versus XC_2. The very good prediction of E(R^2 = 0.688) and σ_{max}(R^2 = 0.836) values is clearly visible. It should be noted that using a standard procedure, vBMD can also be determined from the histogram. However, we need to apply the calibration procedure after <RGL> calculation. Consistently, replacement of vBMD with vBMD/X_2 (Appendix 2) improves the correlations with mechanical parameters. Considering the opportunistic determinations of vBMD(Leonhardt et al., 2020; Löffler et al., 2019; Johannnesdottir et al., 2021; Boutin et al., 20210), our results show that an analysis of RGL histograms should be

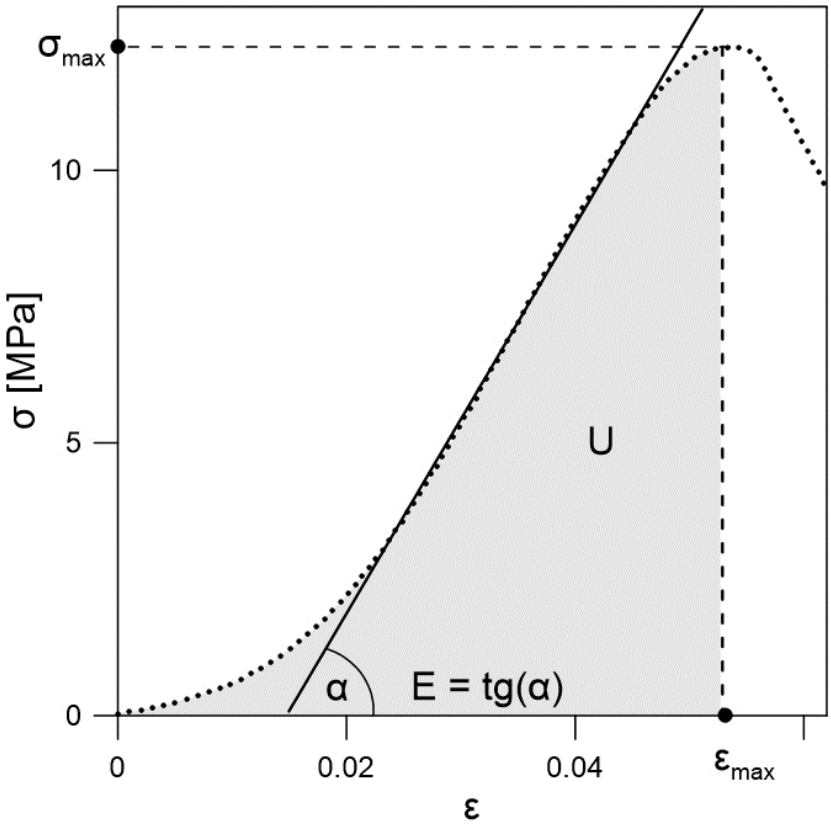

Figure 5: Typical stress-strain (σ-ε) curve obtained during compression of L3 human vertebral body. For the definition of symbols, see text.

performed and the vBMD/X_2 parameter be used to describe the mechanical properties of the vertebrae.

It is worth highlighting two additional advantages of the proposed approach. First, the study describes, in fact, a reanalysis of previously collected data, that is, opportunistic analysis. This confirms the possibility of analysing of CT data acquiring to solve other diagnostic problems. Second, the values of histogram parameters seem to be weakly dependent on the image resolution. The tests performed confirmed that the five-fold deterioration of image resolution (pixel - 730·730 μm^2) changes the parameter values by less than 2%. However, the problem of the image resolution requires additional research using clinical CT data.

Finally, attempts were made to describe the relationship between mechanical parameters and clinically available quantities using the nonlinear models listed above. Based on the values ofR^2, ACI, and BCI, it turned out that the use of a parabolic model provides the best description of E and σ_{max}. The results of the power and logistic models are practically identical to those of the linear model. This is not surprising because using the cellular solid model (Gibson, 2005) the relationships between bone density and mechanical parameters are nonlinear. The advantage of the description using the parabolic function occurs for all parameters characterizing the density.

In the case of XC_2, for E, the values of R^2 are 0.688 and 0.768 for the linear and parabolic models, while for σ_{max} they are equal to0.836, 0.878. Using vBMD/X_2as independent variable, similar values of R^2 were obtained (E = 0.673 and 0.702, σ_{max}= 0.825, 0.837, respectively). For vBMD, R^2 values are E = 0.619 and 0.670 while for σ_{max}= 0.771 and 0.804. It should be noted that ~ (70-90) % of the outcome variables are explained by the parabolic model, while for the linear model, the values R^2 are ~10% lower.

However, one should pay attention to the certain regularity observed in the processing of the results. That is, differences in predictive power between linear and parabolic laws are usually small (<10%) because the ranges of parameter changes exhibited by vertebral bodies are low over 50 years (Tables 1). It is known from mathematics that small changes in variable values can be very accurately described with linear models. Small differences between the results of the parabolic and linear models allow, in our opinion, the use of the linear model in clinical practice.

The studies carried out have several limitations. First, the statistics should be larger. We have analysed 50 vertebral bodies, but the most interesting results were obtained for the group of 18 cases. Increasing the number of subjects studied will probably not change the observed relationships

that appear to be unambiguous. The next drawback is that the examinations were performed *in vitro*. Therefore, the images analysed have provided a better resolution than clinical CT images. Although the test performed showed that the results of the histogram analysis depended weakly on the image resolution, the problem requires further studies. Finally, we should also note the limitations associated with CT. Problems with dose, equipment availability, cost, or lack of reference data (XC_2, $vBMD/X_2$) should also be considered.

Conclusions

In summary, many parameters describing human vertebra were tested as predictors of mechanical properties. This study describes a new method for predicting FR using the parameter extracted from the CT image histogram. In fact, the proposed approach offers a description of the mechanical parameters through the estimator of the bone density. Despite specified above limitations, it seems that the proposed parameter (XC_2) is potentially interesting for *in vivo* applications. Furthermore, it was found that $vBMD/X_2$ provides a better FR estimate than vBMD alone. It should also be emphasized that the proposed method can be used for any abdominal CT performed for other reasons (opportunistic screening).

REFERENCES

Akhter MP, Recker RR (2021). High resolution imaging in bone tissue research-review. Bone. 143:115620, doi:10.1016/j.bone.2020.115620.

Alswat KA (2017). Gender Disparities in Osteoporosis. J. Clin. Med. Res. 9(5): 382-387.

American College of Radiology (2013). ACR-SPR-SSR practice guideline the performance of quantitative computed tomography (QCT) bone densitometry. https://www.acr.org/-/media/ACR/Files/Practice-Parameters/QCT.pdf?la=en.

Boskey AL, Coleman R (2010). Aging and bone. J. Dent. Res. 89(12): 1333-1148.

Boskey AL, Imbert L (2017). Bone quality changes associated with aging and disease: a review. Ann. N Y Acad. Sci. 1410(1): 93-106.

Boutin RD, Hernandez AM, Lenchik L, Seibert JA, Gress DA, Boone JM (2021). CT phantom evaluation of 67,392 American College of Radiology accreditation examinations: implications for opportunistic screening of osteoporosis using CT. Am. J. Roentgenol. 216(2): 447-452.

Checefsky WA, Abidin AZ, Nagarajan MB, Bauer JS, Baum T, Wismuller A (2016). Assessing vertebral fracture risk on volumetric quantitative computed tomography by geometric characterization of trabecular bone structure. Proc. SPIE Int. Soc. Opt. Eng. 9785:978508, doi:10.1117/12.2216898.

Dall'Ara E, Pahr D, Varga P, Kainberger F, Zysset P (2012). QCT-based finite element models predict human vertebral strength in vitro significantly better than simulated DEXA. Osteoporos. Int. 23(2): 563-572.

Demontiero O, Vidal C, Duque G (2012). Aging and bone loss: new insights for the clinician. Ther. Adv. Musculoskelet Dis. 4(2): 61-76.

Diacinti D, Guglielmi G (2019). How to define an osteoporotic vertebral fracture? Quant Imaging Med. Surg. 9(9): 1485-1494.

Engelke K (2017). Quantitative computed tomography – current status and new developments. J. Clin. Densitom. 20(3): 309-321.

Gebre RK, Hirvasniemi J, Lantto I, Saarakkala S, Leppilahti J, Jämsä T (2021). Discrimination of low-energy acetabular fractures from controls using computed tomography-based bone characteristics. Ann. Biomed. Eng. 49(1): 367-81.

Genant HK, Wu CY, Kuijk C, Nevitt MC (1993). Vertebral fracture assessment using a semiquantitative technique. J. Bone. Miner. Res. 8(9):1137-1148.

Gibson LJ (2005). Biomechanics of cellular solid. J. Biomech. 38(3): 377-399.

Hutchinson JC, Shelmerdine SC, Simcock IC, Sebire NJ, Arthurs OJ (2017). Early clinical applications for imaging at microscopic detail: microfocus computed tomography (micro-CT). Br. J. Radiol. 90(1075), doi: 10.1259/bjr.20170113.

Johannesdottir F, Allaire B, Kopperdahl DL, Keaveny TM, Sigurdsson S, Bredella MA, Anderson DE, Samelson EJ, Kiel DP, Gudnason VG, Bouxsein ML (2021). Bone density and strength from thoracic and lumbar CT scans both predict incident vertebral fractures independently of fracture location. Osteoporos. Int. 32(2): 261-269.

Kanis JA, Cooper C, Rizzoli R, Reginster JY (2019). European guidance for the diagnosis and management of osteoporosis in postmenopausal women. Osteoporos. Int. 30(1): 3-44. Erratum in: Osteoporos. Int. 2020, 31(1): 209 and 31(4): 801.

Karim L, Hussein AI, Morgan EF, Bouxsein ML (2013). The mechanical behavior of bone. In: Osteoporosis, Marcus R, Feldman D, Dempster DW, Luckey M, Cauley JA (Eds), Academic Press, Oxford, pp. 431-452.

Kim D, Christopherson GT, Dong XN, Fyhrie DP, Yeni YN (2004). The effect of microcomputed tomography scanning and reconstruction voxel size on the accuracy of stereological measurements in human cancellous bone. Bone 35(6): 1375-1382.

Krug R, Burghardt AJ, Majumdar S, Link TM (2010). High-resolution imaging techniques for the assessment of osteoporosis. Radiol. Clin. North. Am. 48(3): 601–621.

Kubik T, Pasowicz M, Tabor Z, Rokita E (2002). Optimizing the assessment of age-related changes in trabecular bone. Phys. Med. Biol. 47(9): 1543-1553.

Lentle B, Koromani F, Brown JP, Oei L, Ward L, Goltzman D, Rivadeneira F, Leslie WD, Probyn L, Prior J, Hammond I, Cheung AM, Oei EH (2019). The Radiology of osteoporotic vertebral fractures revisited J. Bone. Mineral. Res. 34(3): 409-418.

Leonhardt Y, May P, Gordijenko O, Koeppen-Ursic VA, Brandhorst H, Zimmer C, Makowski MR, Baum T, Kirschke JS, Gersing AS, Seifert-Klauss V, Achwaiger BJ (2020). QCT bone mineral density measurements predicting osteoporotic fractures: a use case in a prospective clinical cohort. Front. Endocrinol. doi:10.3389/fendo.2020.586352.

Leslie WD, Majumdar SR, Morin SN, Lix LM, Schousboe JT, Ensrud KE, Johansson H, McCloskey EV, Kanis JA (2018). Performance of FRAX in clinical practice according to sex and osteoporosis definitions: the Manitoba BMD registry. Osteoporos. Int. 29(3): 759-767.

Liu Y, Wang L, SuY,Brown K, Yang R, Zhang Y, Duanmu Y, Gou Z, Zhang W, Yan C Yan D, Cheng X (2020). CTXA hip: the effect of partial volume correction on volumetric bone mineral density data for cortical and trabecular bone. Arch. Osteoporos. doi:10.1007/s11657-020-00721-8.

Löffler MT, Jacob A, Valentinitsch A, Rienmuller A, Zimmer C, Ryang YM, Baum T, Kirschke JS (2019). Improved prediction of incident vertebral fractures using opportunistic QCT compared to DXA. Eur. Radiol. 29(9): 4980-4989.

López E, Ibarz E, Herrera A, Mateo J, Lobo-Escolar A, Puertolas S, Garcia L (2012). A mechanical model for predicting the probability of osteoporotic hip fractures based on DXA measurements and finite element simulation. BioMed Engineer OnLine, doi:10.1186/1475-925X-11-84.

López Picazo M, Humbert L, Di Gregorio S, González Ballester MA, del Río Barquero LM (2019). Discrimination of osteoporosis-related vertebral fractures by DXA-derived 3D measurements: a retrospective case-control study. Osteoporosis. Int. 30(5): 1099-1110.

Nethander M, Pettersson-Kymmer U, Vandenput L, Lorentzon M, Karlsson M, Mellström D, Ohlsson C (2020). BMD-Related Genetic Risk Scores Predict Site-Specific Fractures as Well as Trabecular and Cortical Bone Microstructure. J. Clin. Endocrinol. Metab. 105(4):e1344–1357.

Shepherd JA, Schousboe JT, Broy SB, Engelke K, Leslie WD (2015). Executive summary of the 2015 ISCD position development conference on advanced measures from DXA and QCT: fracture prediction beyond

BMD. J. Clin. Densitom. 18(3): 274-286.
Silva BC, Broy SB, Boutroy S, Schousboe JT, Shepherd JA, Leslie WD (2015). Fracture Risk Prediction by Non-BMD DXA Measures: the 2015 ISCD Official Positions Part 2: Trabecular Bone Score. J. Clin. Densitom.18(3): 309-330.
Soldati E, Rossi F, Vicente J, Guenoun D, Pithioux M, Iotti S, Malucelli E, Bendahan D (2021). Survey of MRI Usefulness for the Clinical Assessment of Bone Microstructure. Int. J. Mol. Sci. 22(5): 2509. doi: 10.3390/ijms22052509.
Steiger JH (1980). Tests for comparing elements of a correlation matrix. Psychol. Bull 187(2): 245-251.
Tabor Z (2009). Quantifying quality of trabecular bone from low-resolution images. Nalecz Institute of Bio-cybernetics and Biomedical Engineering Polish Academy of Science, Warsaw, pp. 16-56.
Tabor Z, Rokita E (2000). Comparison of trabecular bone architecture in young and old bone. Med. Phys. 27(5): 765-772.
Tarantino U, Iolascon G, Cianferotti L, Masi L, Marcucci G, Giusti F, Marini F, Parri S, Feola M, Rao C, Piccirilli E, Zanetti EB, Cittadini N, Alvaro R, Moretti A, Calafiore D, Toro G, Gimigliano F, Resmini G, Brandi ML (2017). Clinical guidelines for the prevention and treatment of osteoporosis: summary statements and recommendations from the Italian Society for Orthopaedics and Traumatology. J. Orthop. Traumatol. 18(1): 3-36.
Tatoń G, Rokita E, Korkosz M, Wróbel A (2014). The ratio of anterior and posterior vertebral heights reinforces the utility of DXA in assessment of vertebrae strength. Calcif. Tissue. Int. 95(2):112-121.
Tatoń G, Rokita E, Rok T, Beckmann F (2012). Oversampling in the computed tomography measurements applied for bone structure studies as a method of spatial resolution improvement. Pol. J. Radiol. 77(2): 14-18.
Tatoń G, Rokita E, Wróbel A (2013a). Application of geometrical measurements in the assessment of vertebral strength. Pol. J. Radiol. 78(2): 15-18.
Tatoń G, Rokita E, Wróbel A, Korkosz M (2013b). Combining areal DXA bone mineral density and vertebrae postero-anterior width improves the prediction of vertebral strength. Skeletal Radiol. 42(12): 1717-1725.
Valentinitsch A, Trebeschi S, Kaesmacher J, Lorenz C, Loffler MT, Zimmer C, Baum T, Kirschke JS (2019). Opportunistic osteoporosis screening in multi-detector CT images via local classification of textures. Osteoporos. Int. 30(6): 1275–1285.
Xie Q, Chen Y, Hu Y, Zeng Fanwei, Wang P, Xu L, Wu J, Li J, Zhu J, Xiang M, Zeng Fanxin (2022). Development and validation of a machine learning-derived radiomics model for diagnosis of osteoporosis and osteopenia using quantitative computed tomography. BMC Med. Imaging 22(1): 140, doi: 10.1186/s12880-022-00868-5.
Xue Z, Huo J, Sun X, Ai ST, Zhang L, Liu C (2022) Using radiomic features of lumbar spine CT images to differentiate osteoporosis from normal bone density. BMC Musculoskelet Disord. 23: 336, doi:10:1186/s12891-022-05309-6.
Yamada S, Chiba K, Okazaki N, Era M, Nishimo Y, Yokota K, Yonekura A, Tomita M, Tsurumoto T, Osaki M (2019). Correlation between vertebral bone microstructure and estimated strength in elderly women: an ex-vivo HR-pQCT study of cadaveric spine. Bone. 120(3): 459-464.
Yan J, Lai Y, Xu Y, Zhen Y, Niu Z, Tan T (2023). Artificial intelligence-based medical image automatic diagnosis and prognosis prediction. Front. Phys. doi:10.3389/fphy3023.1210010.

Cite this article as:
Rokita E, Wróbel A, Tatoń G (2024). Improved prediction of bone mechanical parameters based on clinically available CT data. 12(1): 001-011

Submit your manuscript at
http://www.academiapublishing.org/journals/mms

APPENDIXES

Appendix 1

The definitions of mechanical parameters are given in Fig. 5. E, σ_{max}, ε_{max} and U/V are elastic modulus, ultimate stress ($\sigma_{max} = F_{max}/A$: F_{max}- maximum load, A – axial cross section area at the narrowest site of the vertebral body), ultimate strain ($\varepsilon_{max} = \Delta L/H$: ΔL – failure displacement, H – average height of the vertebral body) and work to fracture (U) divided by the volume of the vertebral body (V), respectively. It should be noted that forthe vertebral body, the stress–strain curve exhibits nonlinearity at low stress levels, and care must be taken to calculate the parameters in a manner that is standardized across samples.
Assuming that the vertebral body is a cylinder with the volume V = A·H, made of a material that meets Hook's law ($\sigma = E \cdot \varepsilon$), one can calculate the energy storage in the elastic body:

$$U = \int_0^H F dH' = \int_0^{\varepsilon} (\sigma \cdot A) d(\varepsilon' H) = V \cdot \int_0^{\varepsilon} \sigma d\varepsilon' \approx V \frac{1}{2} \sigma_{max} \cdot \varepsilon_{max}$$

The last approximation is valid since the vertebral body resembles a ceramic material. The maximum stress appears only a little into the nonlinear elastic region. Using Hook's law,the following approximation can be used:

$$\varepsilon = \frac{\sigma}{E} = const \rightarrow \varepsilon_{max} \approx \frac{\sigma_{max}}{E}$$

which further approximates U/V as:

$$\frac{U}{V} \approx \frac{1}{2} \sigma_{max} \cdot \varepsilon_{max} = \frac{\sigma_{max}^2}{2E}$$

The correctness of the approximation used is confirmed by a very strong correlation between U/V and $(\sigma_{max})^2/2E$ ($r = 0.94$, $p < 0.0001$). The relations described above make it possible to limit the description of the mechanical property of a vertebral body to two parameters.

Appendix 2

In our approach, a patient-specific phantom-less normalization method was applied. The technique uses the patient's own internal tissue (average ROI^{IS} grey level – <GTC>, Figure 1) as normalization material. This makes it possible to replace GLT (ROI^{T}, Figure 1) with RGL = GLT/<GLC>. It should be noted that the GL values within ROI^{T} and ROT^{IS} are determined during the same CT examination and both regions are close to each other (~cm). Therefore, the influence of all parasitic effects, characteristic for CT examination, on GL value is practically identical. The use of RGL is a simple method to limit the influence of the operating parameters of the X-ray tube, the radiation hardening effect, the image processing method, etc.
Assuming that the vertebral body is composed of two phases (organic matrix – 1 and bone material - 2) and using the rule of mixture, the following formula may be written:

$$\rho = \rho_1 \cdot v_1 + \rho_2 \cdot v_2 = vBMD \approx C \cdot (XC_1 \cdot X_1 + XC_2 \cdot X_2)$$

where ρ is density of trabecular bone (vBMD), ρ_1 and ρ_2 are densities of both phases while v_1 and v_2 are the normalized volume fractions ($v_1 + v_2 = 1$) and C is constant. The XC_1 and XC_2parameters are linearly related to organic matrix and bone material densities. The X_1 and X_2 are organic matrix and bone material normalized volume fractions. The parameters SD_1 and SD_2 reflect bone material and organic matrix distributions.
It should be noted that in the standard approach vBMD is calculated using a calibration curve based on the average RGL value (<RGL>). As expected, a very strong vBMD-<RGL> correlation was observed ($r = 0.97$, $p < 0.0001$). By performing histogram analysis (Figure 2), the contribution of the organic phase (X_1) and the mineral phase (X_2) is separated and the quantities that measure the density of the individual phases (XC_1 and XC_2) are determined.
Also, the following approximation can be used:

$$\frac{vBMD}{X_2} = C \cdot (XC_1 \cdot \frac{X_1}{X_2} + XC_2) \approx C \cdot XC_2$$

Correctness of the approximation is confirmed by very strong correlation of $vBMD/X_2$ and XC_2 ($r = 0.90$, $p < 0.0001$).